FED-Vol. 221, Industrial and Environmental Applications
of Fluid Mechanics
ASME 1995

ANALYSIS OF PRESSURE TRANSIENTS IN CCW PIPING DUE TO PUMP STARTUP FOLLOWING A SAFETY INJECTION SIGNAL

Rupak. K. Banerjee Ph.D.
Jaipal S. Rathi Ph.D.

Raytheon Engineers and Constructors
Fluid Analysis Group
30th South 17th Street
Philadelphia, PA 19104

INTRODUCTION

During testing of a Component Cooling Water System (CCWS), high pressures due to startup of a Compnent Cooling Water (CCW) pump have been observed. The high pressure exceeded the system set pressure and resulted in lifting and damage of pressure relief valve (PRV). The objective of this analysis is to quantify and determine the cause of maximum transient pressure generated by the CCW pumps startup after a safety injection (SI) signal in the event of a loss of offsite power (LOOP).

In past studies, generally, it has been observed that the transient pressure surge, solely due to pump start-up, is insignificant for the purpose of water hammer analysis. It has been found that the pressure rise due to pump start up can reach within a few percent of pump shut-off head. In contrast, for the CCWS studied here, it has been observed that an unusual high pressure spike, approximately two times the pump shut-off pressure, is measured whenever a CCW pump is started. This phenomenon is observed repeatedly and with disregard to any time delay between repeated attempts of CCW pump startup.

Because of the nature of the piping layout, it has been observed that there are several high points in the system where air can accumulate during shutdown or outage periods. Any existing air pockets can augment to the severity of hydraulic transients. This analysis accounts for the presence of trapped air at those locations where air has been found to be present during the field test. Since the amount of air could not be accurately determined in the field test, the impact of air pockets need be determined parametrically.

BACKGROUND

In the past many authors have studied the wave propogation phenomenon in various piping configuration and for different boundary conditions to undrstand the reason for pressure surge. Head rise resulting from compression of entrapped air has been demonstrated by Wylie and Streeter (1978). For a simple system they have showed the increase in velocity before the head rise is significant. The numerical solution to the differential equations of continuity, momentum and thermodynamic gas response clearly shows that entrapped air may prove to be either detrimental or beneficial, depending upon the amount and location of the air as well as the pipeline configuration and the nature and cause of the transient (Martin, 1976). In other words, the cause of a pressure surge in a piping system need to be addressed on a case by case basis. Using the method of characteristics, Provoost (1976) calculated and experimentally verified the pressure surge due to column-separation at high points in a prototype pipeline.

In order to understand the cause of pressure spike due to pump startup in a CCW loop, a review of the system description is required. CCWS in a nuclear power plant is a part of Auxiliary Cooling System (ACS). The CCWS is a closed loop, non-radioactive, and controlled chemistry cooling water system. The main function of the CCWS is to provide an intermediate or interfacing/separation function between the Service Water System (SWS), which is non-redioactive ultimate heat sink having direct contact with the environment, and the component being cooled. Generally, the component being cooled with CCW interface is a radioactive system, such as the residual heat removal heat exchanger (RHR Hx), which has reactor coolant on the tube side and CCW on the shell side. With this arrangement, the CCWS provides additional assurance against release of radioactive cooling water to the environment via the SWS, if there is a failure of the heat exchange apparatus interfacing with the radioactive component/system being cooled.

Since the CCWS supports Engineered Safety Feature (ESF) Systems, e.g, RHRS, by providing the cooling function, this system is considered part of, or one of, the ESF Systems. Accordingly, the CCWS is required for accident mitigation, and is functional or available for operation during the design basis events, e.g., loss of offsite power (LOOP) or loss of coolent accident (LOCA) with a single active or passive failure.

FLOW CONDITIONS

A simplified flow diagram of a CCWS is shown in Figure 1. The CCW basically consists of three CCW pumps, two CCW and RHR heat exchangers, and two independent supply/return piping circuits with surge tanks on the pump suction side. Cross-connections with isolation valves are provided at the CCW pump suction and discharge, and at the CCW Hx's discharge header for splitting the CCWS into two independent loops. Two independent

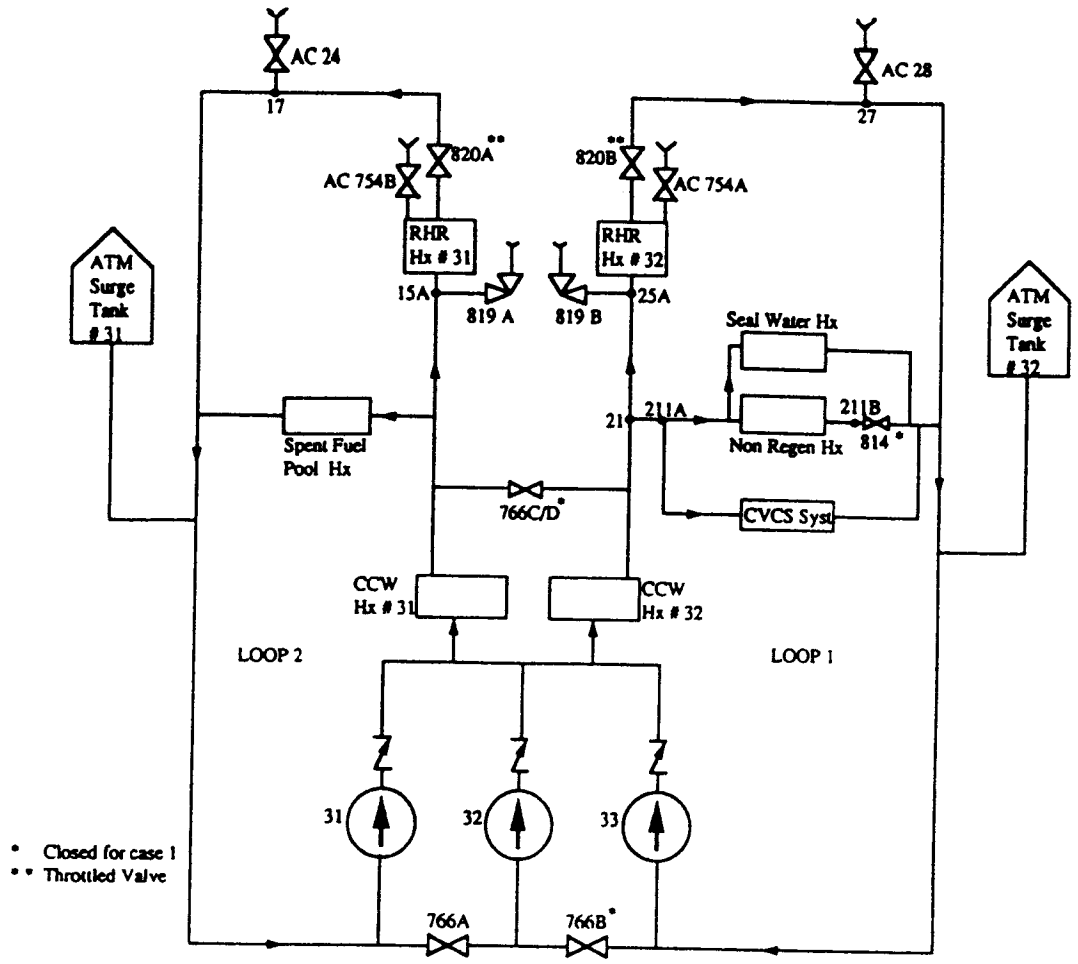

FIG. 1 Schematics of CCW Flow Loop

surge tanks are connected to the respective side of the CCW pump suction header to accomodate system volume changes as a result of thermal expansion and contraction, and to provide net positive suction head (NPSH) to the CCW pumps. The surge tanks also allow for operator reaction time to changes in volume as a result of leaks into or out of the system, the sufficient volume to allow continuous system operation until a small leak can be isolated.

For the present study, two scenarios have been analyzed. Case 1 simulates the test condition during outage period whereas Case 2 address the restart of the CCW pumps following a trip due to occurrence of a SI signal with LOOP. Water temperature is taken to be 80° F. Following cases have been analyzed:

Case 1: One Loop Operatoion- A Test Scenario

The test scenario analyzed is as follows:

- o One loop with RHR heat exchanger 32 is in operation.
- o Pump 33 starts after tripping due to a SI signal
- o In order to isolate the two CCW loops, valves AC-766B, AC-766C, and AC-766D are in closed position.
- o Valve 814 downstream of Nonregenerative heat exchanger is closed.
- o Air pockets are present at the top of the RHR heat exchanger, at Valves AC-24 & Ac-28, and upstream of the Valve 814 (as observed during test condition).

Case 2: Two Loop Operaation- An Operating Scenario

The scenario analyzed is as follows:

- o Both CCW loops are in operation.
- o Pump 31 starts first at t= 0 second and 5 seconds later pumps 32 and 33 starts simultaneously).
- o Valve 766B, 766C, and 766D are open.
- o Valve 814 downstream of Nonregenerative heat exchanger is open and no air is present in the piping.

METHOD OF ANALYSIS

A hydraulic model of the system, schematically shown in Figure 1, has been developed to analyze the transients using LIQT computer program (1990). LIQT calculates the transients pressures and flows in liquid water systems using the method of characteristics and properly accounts for the effects of non-condensible gases. The startup of a pump is achieved using motor torque, motor/pump inertia and pump characteristics.

Pipe Friction Factors

Figure 1 shows the major users of CCWS along with some of

the important nodes. The piping between any two consecutive nodes is designated as a link. In order to calculate the overall loss factor (K-factor) for each link, first various loss parameters (pipe length, fittings, valves, etc.) appropriate to the link are listed. These parameters are then input to the interactive computer code PIPEFLOW (1991) which calculates flow coefficient (Cv) for each link. The Cv of each link is then converted into the corresponding overall K-factor [= 891 d^4/C_v^2 (1986) where d is diameter of pipe in inch]. The loss factor K is further converted into an equivalent friction factor, f [= KD/L (1986) where L and D are diameter and length of pipe in feets] as required by the computer code LIQT. The combined K-factor, nodal elevation, pipe diameter, pipe length (actual as well as adjusted, where required), and the calculated equivalent friction factor are listed in Table 1.

Where link lengths are short (less than about 4.25 ft.), it is necessary to modify the length based on the wave speed in order to satisfy computational requirements. Minor users requiring small flow rates carried in small diameter (3 in. and lower) piping are not included as they won't have a significant effect on the hydraulic transient results.

Component Loss factors

Valve settings are based on the CCWS Flow Balance Test. Valves 820A and 820B, downstream of RHR Hxs, are 22% and 28% open, respectively. The K-factors of the throttled butterfly valves 822A, 822B, and 803 are based on generic valve characteristics derived from Fisher (1991) and Neles-Jamesbury (1991) catalogs. Other fully open valve Cvs (not shown in Figure 1) are based on generic data from RE&C Special Report SR-301 (1983). The hydraulic resistance factors of the CCW Hxs and RHR Hxs are based on test data. Hydraulic resistances of side stream branches are adjusted to match the test flow.

Speed of Sound

The speed of sound is calculated from the following formula [LIQT (1990)]:

$$a = \{(K^*g/rho)/[1+(K/E)(D/e)]\}^{0.5}$$

where,

E = Modules of elasticity of steel, lb/sq. in
K = Bulk Modules of fluid, lb/sq. in.
rho = density for water, lbm/cu. ft
D = diameter of pipe, ft
e = wall thickness, ft

Pump and Motor Characteristics

The CCW pump and motor characteristics are obtained from vendor supplied data. The head vs. flow data for the pump are as follows:

Head, ft	312	306	300	290	288	278	260	232
Flow, gpm (x1000)	0	4	8	12	16	20	24	28

The moment of inertia of the pump-motor assembly, the rated torque and the specific speed of the pump are calculated based on LIQT program. These data are used to generate the pump file which is used in the transient analysis. For simulating the pump startup a generic speed-torque curve for an induction motor is used from LIQT program.

TABLE 1: Combine K-factor for Links, Nodal Elevations, Pipe Diameter and Length, and Equivalent Friction Factors

NODE A	NODE B	ELEV. ft.	DIA. inch.	Cv	K	Act. L ft.	Mod.L ft.	f(mod)
310	311	43.29	10.02	1934.6	2.399751	32.08	32.08	0.062462
311	312	50.79	10.02	2423.2	1.529573	25.94	25.94	0.049236
312	C31U	76.73	13.25	4026	1.694313	10.08	12.5	0.149664
P320	321	43.29	10.02	1850.7	2.622265	34.77	34.77	0.062974
321	322	50.79	10.02	2360.6	1.611773	25.94	25.94	0.051882
P330	331	43.29	10.02	1702.9	3.097207	38.27	38.27	0.067577
331	332	47.08	10.02	2207.6	1.842926	32.9	32.9	0.046773
332	C32U	76.73	13.25	7584.9	0.477355	8.25	8.5	0.062009
322	312	76.73	13.25	13319	0.15481	4.46	4.46	0.038326
322	332		10.02	3045.4	0.968411	3.71	4	0.202156
C32D	20	58.75	13.25	4799.9	1.192002	18.42	18	0.07312
20	21	48.5	15.25	4321.5	2.580406	47.17	47.17	0.06952
21	22	48.5	13.25	4271.1	1.505434	64.33	64.33	0.025839
22	23	59.5	13.25	4539.2	1.332854	51.58	51.58	0.028532
23	24	59.5	12	2093.1	4.217186	88.08	88.08	0.047879
24	25	54.5	12	3339	1.657181	74.29	74.29	0.022307
25	25A	48.42	12	3689.7	1.357127	32.23	33.6	0.040391
25A	R32U	63.75	12	5686	0.571464	28.04	29	0.019706
R32D	26	63.71	12	2501.7	2.952108	95.92	95.92	0.030777
26	27	46.92	12	2454.6	3.066488	127.83	127.8	0.023989
27	28	56.5	13.25	3729.5	1.974422	75.67	75.67	0.028811
28	29	45	15.25	4883.7	2.020501	10	8.5	0.302085
29	30	47	15.25	9588.3	0.524172	4.72	4.25	0.156738
30	31	49.14	15.25	4844.7	2.053162	11.06	12.5	0.208738
32	31	49.14	12	5442.1	0.623835	4.65	4.5	0.13863
32	P31S	49.14	12	3381	1.616264	25.48	25.48	0.063433
31	P32S	49.14	12	3434.1	1.566667	19.13	19.13	0.081896
30	P33S	49.14	12	3115.6	1.903353	19.26	19.26	0.098824
C31D	10	58.75	13.25	5583.6	0.880872	13.88	13.5	0.072047
10	11	48.5	15.25	4361.5	2.533292	63.88	63.88	0.050398
11	11A	51.17	13.25	4978.7	1.107922	28.5	28.5	0.042924
11A	12	50.17	12	3762.1	1.305395	36.25	36.25	0.036011
12	13	64	12	4155.7	1.069829	50.42	50.42	0.021218
13	14	64	12	2921.8	2.164222	61.08	61.08	0.035433
14	15	47	12	2977	2.084707	98.9	98.9	0.021079
15	15A	47	12	4793.9	0.803942	21.81	21.81	0.036861
15A	R31U	58.02	12	3353.2	1.643175	46.2	46.2	0.035567
R31D	16	69.71	12	2202.2	3.809686	116.8	116.8	0.032617
16	17	49	12	2314.5	3.448961	135.08	135.1	0.025533
17	17A	64	12	2153.5	3.983941	41.75	41.75	0.095424
17A	18	46.75	13.25	3801.2	1.90064	37.96	37.96	0.055285
18	19	46.75	15.25	7559.5	0.843278	20.15	20.15	0.053184
19	32	51.47	15.25	11762	0.348333	14.33	13.25	0.033409
10	20	48.5	12	7532	0.325673	6	8.2	0.039716
ST1	19	81	4.03	208.8	5.390597	61.13	61.13	0.029615
ST2	29	81	4.03	190.1	6.503298	69.75	69.75	0.031312
21	211A	48.5	10.02	3135.8	0.913381	38.33	38.33	0.019898
211A	211	60	10.02	3862.7	0.601959	15.17	16	0.031415
211	NRU	74.17	6.065	580.7	3.575175	51.33	52	0.034749
NRD	214	78.5	6.065	477.6	5.285332	53.25	52	0.051371
211	212	74.17	7.981	299.2	40.38162	33.67	33.67	0.797658
212	SMU	88.5	3.068	82.9	11.48656	86.34	86.34	0.034014
SMD	213	77.67	3.068	93.2	9.087979	71.75	71.75	0.032383
213	214	87.5	7.981	1647.8	1.331367	31.91	31.91	0.027749
214	215	74.17	10.02	3537.5	0.717721	15.16	16	0.037456
215	28	60	10.02	2007	2.229738	40.68	40.68	0.045768
11A	SMDU	50.08	7.981	1315	2.090525	16.21	16.21	0.085773
SMDD	17A	60.83	7.981	563.9	11.36849	49.88	49.88	0.151584
211A	221	60	3.07	31.5	79.76458	20.31	20.31	1.004748
221	CPDU	69.5	2.07	50.1	6.517539	41.15	41.15	0.027321
CPDD	222	56.82	2.07	45.1	8.042777	39.69	39.69	0.034955
222	215	69.5	3.07	119.3	5.560967	20.48	20.48	0.069467

Air Pocket

The hydraulic model appropriately accounts for the presence of air pockets at various points in the system. At the time of pump startup, the system would have accumulated some air. The

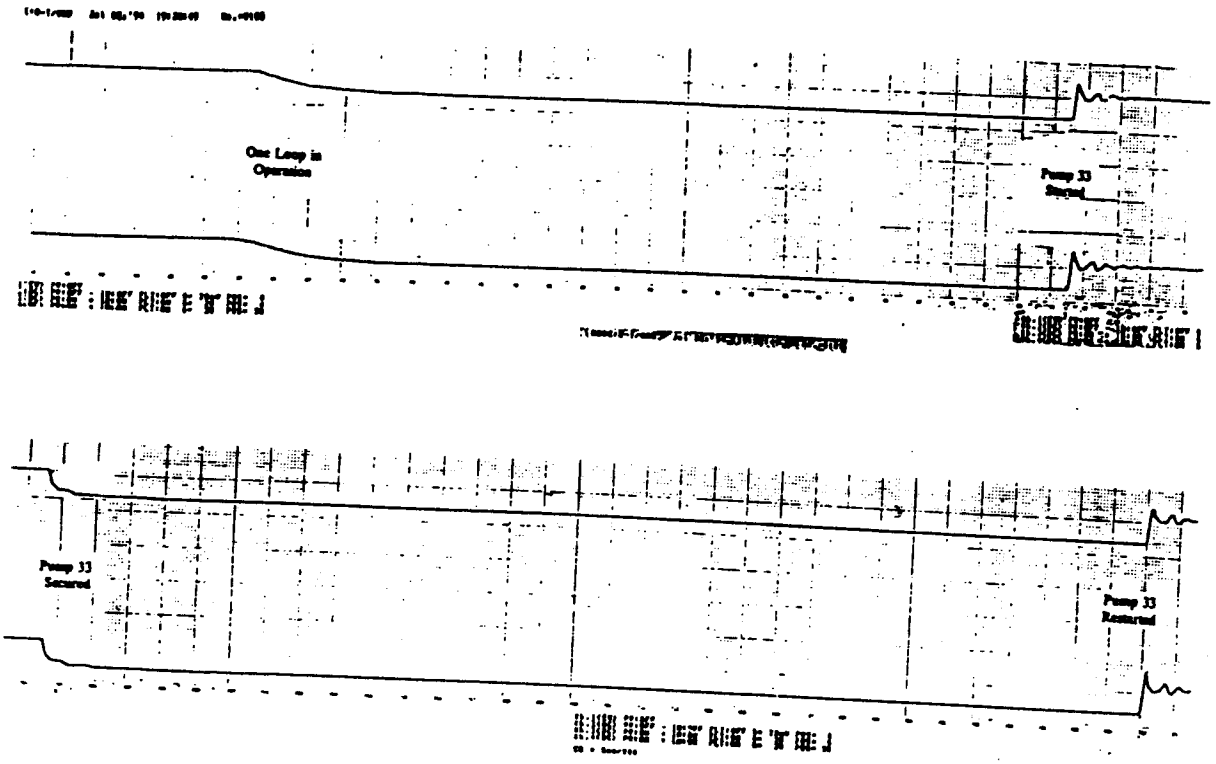

FIG. 2: Pressure-time history at the relief valve location, node #25A, for one loop operation (Case 1 - a test scenario). The relief valve lifted and reached a pressure of 172 psig.

locations where air has accumulated are taken to be only those where air is observed, as recorded in the test. According to the test, air was observed at AC-24, AC-28, AC-754A, and AC-754B. It is assumed that air is not present at any other location. Since the exact amount of air present is not known, the analysis determines the impact of air, parametrically.

RESULTS

The results for Case 1 and Case 2 are as discussed below:

Case 1

Figure 2 shows the experimental measurement of pressure surge in Loop 1 due to repeated start up of pump 33. In one loop operation and system configuration identical to that used in the field test, the calculated maximum pressures due to startup of Pump 33 are presented in Table 2A. Based on test results approximate volumes of 0.05 cu. ft. for the air pockets are assumed at the top of RHR Hxs as well as at Valves AC-24 and AC-28. The air pocket volume upstream of the closed valve 814 is varied from 0 to 1.0 cu. ft. parametrically.

It is seen that as the volume of air reduces at valve 814 the peak calculated pressure also drops (cases 1b to 1e). However, if the air pocket is too large, the peak pressure actually decreases as seen from the comparing cases 1a and 1b. Figures 3a through 3e show the pressure-time histories.

The maximum pressure in one-loop configuration, identical to the one used in the filed test is calculated to be 172 psig. Since the relief valve set pressure is 150 psig, the transient pressure will result in lifting of the relief valve 819B as observed in the test. The high pressure spike appears to have been generated by an air pocket trapped against the closed Valve 814. For case 1b, propogation of

TABLE 2A: Maximum Pressure and Time at PRV for Case 1

Case No.	Air Volume at Non-Regen Hx (cu. ft.)	Safety valve 819A Node # 15A		Safety valve 819B NODE # 25A	
		Pressure (psig)	Time (sec.)	Pressure (psig)	Time (sec.)
1a	1.00	165	1.12	162	0.98
1b	0.75	146	1.06	172	0.90
1c	0.50	120	1.48	155	0.82
1d	0.25	121	0.75	143	1.08
1e	0.0	119	0.62	98	1.04

TABLE 2B: Reduction in Peak Pressure from Node 211B to 15A for Case 1

Node #	211B	211A	25A	15A
Pressure, Psig	490	230	172	146

pressure wave with time and distance from the side-stream piping with entrapped air (node #211B to 211A) to the relief valve locations in the main-stream piping (node #25A to 15A) is shown by arrow #1 in Figure 3f. Table 2B shows the reduction in peak pressure of 490 psig at node #211B to a value of 146 psig at node #15A. Clearly the pressure surge has originated at the side-stream piping having entrapped air, and when it has reached the main-

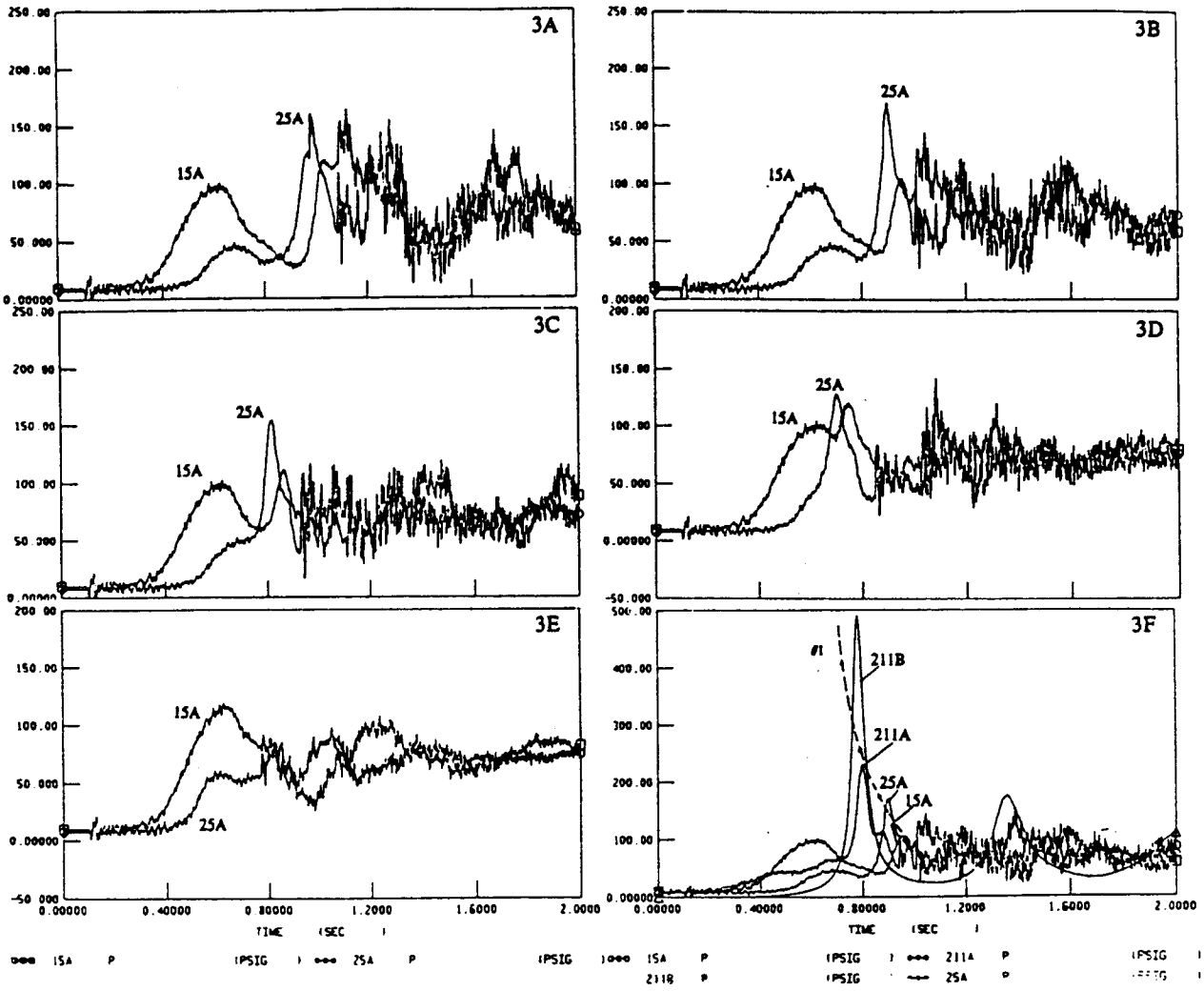

FIG. 3A-3F: Pressure-time history with different volumes of air (1 ft³ for Fig. 3A, 0.75 ft³ for Fig. 3B, 0.5 ft³ for Fig. 3C, 0.25 ft³ for Fig. 3D, 0.0 ft³ for Fig. 3E) at Non-Regen. Hx., one CCW train in operation, one pump startup at t= 0 sec. 0.05 cu. ft. of air at both RHR Hx and valve AC24/28. Valve 814 is closed. For case 1b, propogation of pressure wave with time and distance from node #211B-211A-25A-15A) is shown by arrow #1 in Figure 3F.

stream piping, the magnitude of peak pressure has reduced with time and distance.

TABLE 3: Maximum Pressure and Time at PRV for Case 2

Case No.	Air Volume at each RHR Hx & valve AC24 & AC28 (cu. ft.)	Safety valve 819A Node # 15A		Safety valve 819B NODE # 25A	
		Pressure (psig)	Time (sec.)	Pressure (psig)	Time (sec.)
2a	0.0 [Note 1]	149.8	6.0	149.2	6.0
2b	0.05 [Note 1]	150.2	6.0	142.4	6.2
2c	0.2 [Note 1]	142.6	6.2	128.7	6.1

Case 2

For two-loop operation with valve 814 open and air pockets at the top of RHR heat-exchangers and at valves AC-24 and AC-28, the calculated peak pressures are provided in Table 3. The maximum pressure occurs due to the startup of second and third pump simultaneously. The effect of air at the top of RHR heat exchangers and at valves AC-24 and AC-28 is not significant. Figures 4a through 4f show the pressure-time histories.

In the two-loop operation model the valve 814 is open and no air pocket is postulated. The maximum pressure in the two loop operation is calculated is 150 psig.

SUMMARY AND CONCLUSIONS

This analysis has demonstrated that the maximum pressure in one-loop operation with air pocket present at the closed valve 814 can be significantly higher than the relief valve set pressure of 150 psig, depending upon the size of the air pocket. The results show

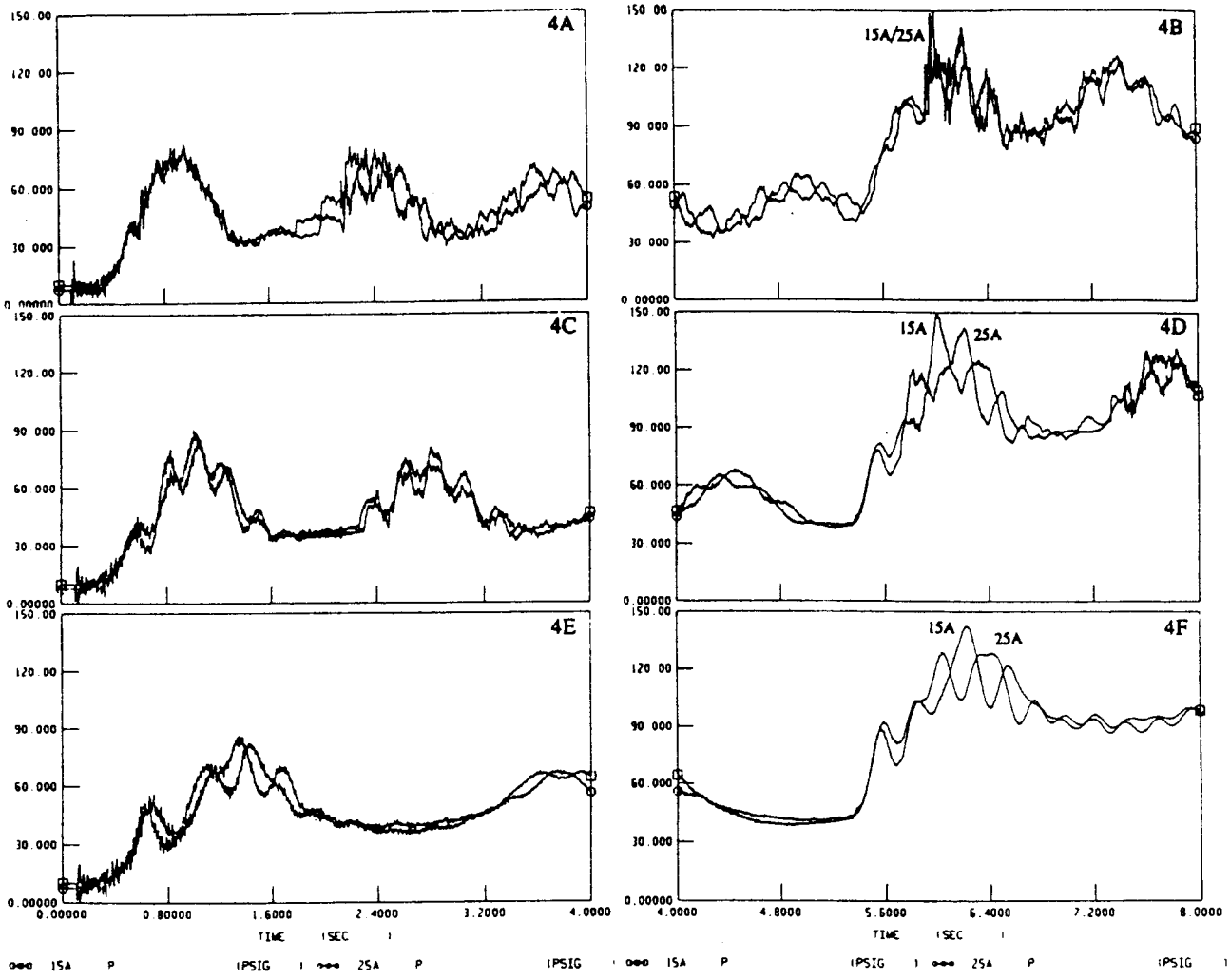

FIG. 4A-4F: Pressure-time history from 0 to 8 sec (with no air for Fig. 4A and 4B, 0.05 ft^3 air for Fig. 4C and 4D, and 0.2 ft^3 air for Fig. 4E and 4F in both RHR Hx and near valve AC24/28), both CCW train in operation, one pump start at t= 0 sec and other two pumps start at t= 5 sec.

that the maximum pressure peaks around 172 psig. It is interesting to note that a pressure of 175 psig was recorded in the field test (Figure 2) and this resulted in lifting of relief valve 819B. The maximum transient pressure due to a pump start up in one- loop operation with Valve 814 closed and no air pocket upstream of the valve is significantly lower than the relief valve set pressure. From this it is obvious that when Valve 814 is open the transient pressure would be even lower.

In two-loop operation the peak pressure may reach the relief valve set pressure. However, since the maximum pressure (150.2 psig) is too close to the set pressure and the duration of this maximum pressure is typically very short, the relief valve, either may open momentarily and then sit back or may not open at all. In either case the system is expected to function satisfactorily.

Hence, it is to be noted that the situation, where valve, such as 814, is closed resulting in a dead-ended pipe and has air pocket upstream of it, may result in maximum transient pressures well in excess of the relief valve set pressure, as indicated from the results of Case 1. Therefore, if a valve is closed for any reason, the line upstream of it must be kept free of air.

REFERENCES

Wylie, E. B., and Streeter, V. L., 1978, Fluid Transients, McGraw-Hill International Book Co., Chapter 8, pp 136-155.

Martin, C. S., 1976, Entrapped Air in Pipelines, Proc. 2nd Int. Conf. Pressure Surges, Bedford, England, BHRA.

Provoost, G. A., Investigation into Cavitation in a Prototype Pipeline Caused by Water Hammer, Proc. 2nd Int. Conf. Pressure Surges, Bedford, England, BHRA.

LIQT - Liquid Transient Analysis Program, 1990, Stoner Associates, Inc., Version 6.0.

RE&C Computer Program PIPEFLOW, 1991, Version 3, Rev.0.

CRANE Technical Paper No. 410, 1986, Flow of Fluids through Valves, Fittings, and Pipe.

Mark's Standard Handbook of Mechanical Engineers, 9th Ed., McGraw-Hill.

FISHER Catalog 10, 1991, Sec.1.

Neles-Jamesbury Technical Information Bulletin T150-1, 1991.

RE&C Special Report SR-301, 1983, Hydraulic Loss Factors for Piping Components.